A Real Time QRS Detection Using Delay-Coordinate Mapping for the Microcontroller Implementation

Article *in* Annals of Biomedical Engineering · February 2002

DOI: 10.1114/1.1523030 · Source: PubMed

5 authors, including:

Jeong-Whan Lee
Konkuk University
107 PUBLICATIONS **949** CITATIONS

SEE PROFILE

Byungchae Lee
Yong-in Songdam College
9 PUBLICATIONS **221** CITATIONS

SEE PROFILE

Annals of Biomedical Engineering, Vol. 30, pp. 1140–1151, 2002
Printed in the USA.

0090-6964/2002/30(9)/1140/12/$15.00

A Real Time QRS Detection Using Delay-Coordinate Mapping for the Microcontroller Implementation

JEONG-WHAN LEE,[1] KYEONG-SEOP KIM,[2] BONGSOO LEE,[2] BYUNGCHAE LEE,[3] and MYOUNG-HO LEE[4]

[1]M_Application Project Team, Samsung Advanced Institute of Technology, Suwon, Korea; [2]School of Biomedical Engineering, College of Medicine, Konkuk University, Chungju, Korea; [3]Department of Medical Information System, Yong-in Songdam College, Yongin, Korea; and [4]Department of Electrical and Computer Engineering, Yonsei University, Seoul, Korea

(Received 30 September 2001; accepted 6 August 2002)

Abstract—In this article, we propose a new algorithm using the characteristics of reconstructed phase portraits by delay-coordinate mapping utilizing lag rotundity for a real-time detection of QRS complexes in ECG signals. In reconstructing phase portrait the mapping parameters, time delay, and mapping dimension play important roles in shaping of portraits drawn in a new dimensional space. Experimentally, the optimal mapping time delay for detection of QRS complexes turned out to be 20 ms. To explore the meaning of this time delay and the proper mapping dimension, we applied a fill factor, mutual information, and autocorrelation function algorithm that were generally used to analyze the chaotic characteristics of sampled signals. From these results, we could find the fact that the performance of our proposed algorithms relied mainly on the geometrical property such as an area of the reconstructed phase portrait. For the real application, we applied our algorithm for designing a small cardiac event recorder. This system was to record patients' ECG and R–R intervals for 1 h to investigate HRV characteristics of the patients who had vasovagal syncope symptom and for the evaluation, we implemented our algorithm in C language and applied to MIT/BIH arrhythmia database of 48 subjects. Our proposed algorithm achieved a 99.58% detection rate of QRS complexes. © *2002 Biomedical Engineering Society.* [DOI: 10.1114/1.1523030]

Keywords—QRS complexes, Reconstructed phase portrait, HRV, ECG.

INTRODUCTION

The electrocardiogram (ECG) signal that is an electric activity generated by a heart has been used as a primary method for diagnosing the abnormal condition of a heart. With the semiconductor technology advancement, microprocessors are adopted to implement a portable or ambulatory ECG monitor as a primary signal-processing device for detecting arrhythmia by evaluating ECG signals. However, the performance of ECG monitor highly depends on the reliable QRS complex detection ability. There has been much research to devise the accurate and fast QRS detection algorithms by either a linear or a nonlinear digital filter with adopting rule-based decisions[3,6,16,17,19,28] or wavelet transforms.[5,7,12,20] Hamilton[6] motivated the researchers by inventing the numerous QRS detection algorithms and his algorithms are widely applied into implementing a portable or ambulatory ECG event recorder. Due to the recent advance in digital technology, it is possible to implement digital filters more densely into a single digital signal processor (DSP).[5,19] Although a single DSP based ECG event detector with the high detection rate of QRS event is desirable, the size and power consumption of the device is not appropriate for both ambulatory and home use. To comply with the constant needs for implementing an efficient ECG event detection algorithm on the small cardiac event-recording devices, a compact and simple ECG event recorder is required to measure heart rate variability (HRV) in real time.

An important part of our work was to develop a QRS detection algorithm, which is small in code size, accurate in QRS detection even in noisy environment, and especially feasible for small microcontrollers. To achieve our goal, we adopted the nonlinear dynamics method derived from chaos physics that reconstructs a phase portrait. This method was proposed initially by Shaw[26] and Takens.[27] They showed that a phase portrait topologically equivalent to a given dynamical system could be reconstructed by successive measurements with a single variable of the system. Several investigations[1,8,18] applied this technique to analyze the electrocardiograph data. Recently, many researchers had been concentrated on analyzing the chaotic characteristics of ECG signal but they missed the fact that the phase portrait reconstruction method could give us a new point of interpreting and visualizing the ECG signal. From the phase portrait of the ECG signal, we could find the specific characteristics of QRS complexes that generate specific trajectories related with ECG components such as P and T wave. To distinguish the QRS complex from the other wave com-

Address correspondence to Kyeong-Seop Kim, Ph.D., School of Biomedical Engineering, College of Medicine, Konkuk University, 322 Dan Wall Dong, Chungju 380-701, Korea. Electronic mail: kyeong@kku.ac.kr

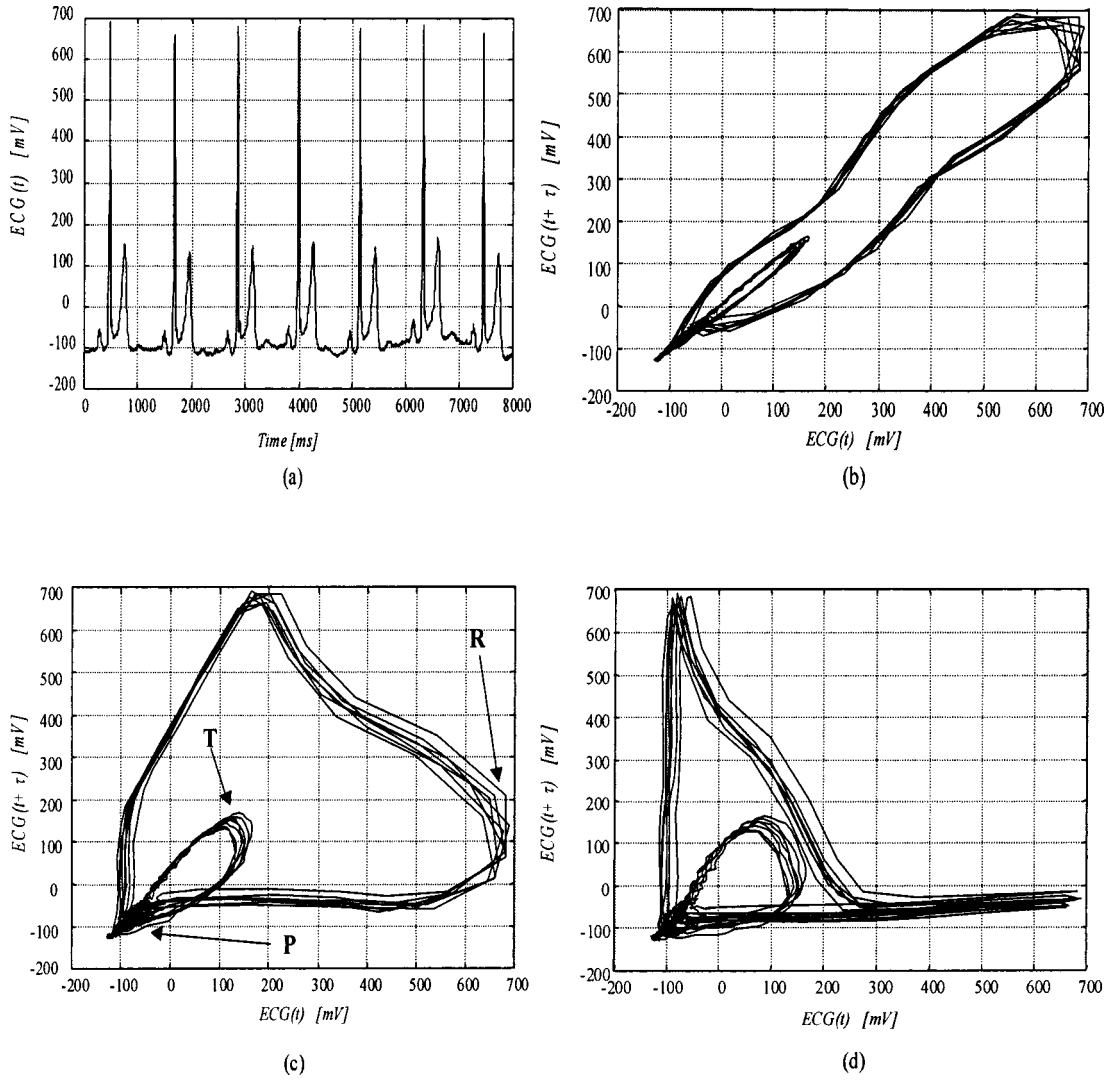

FIGURE 1. The phase portraits of ECG signal with various time delays: (a) sampled ECG signal; (b) phase portrait of ECG signal with time delay, 8 ms; (c) phase portrait of ECG signal with time delay, 20 ms; (d) phase portrait of ECG signal with time delay, 40 ms.

ponents, we utilized the geometrical property of the QRS complex. Compared with the other detection schemes, our method is mainly characterized by two-dimensional vector trajectories and by the simplified preprocessing stages for localizing QRS complex energy. In general, the preprocessors include a successive of band-pass filtering, differentiation, square law detection, and moving-average filtering. In our proposed algorithm, we adopted only a low-pass filtering and delay coordinate utilizing lag rotundity. To locate the QRS complex, we computed the area of phase portrait drawn into a new phase space domain.

Delay-Coordinate Mapping

The embedding method, initially adopted by Takens[27] is a standard way of reconstructing an attractor from a sampled time series in one state component. It is well known that the behavior of a dynamic system can be described by the differential equations. After the transient behavior has decayed, the typical phase trajectories approach a limited set of ''attractors'' that govern the behavior of the dynamic system. Unfortunately, this set of attractors cannot be seen directly; instead, only a sequence of scalar measurements (for instance, a voltage or a component of fluid velocity) can be recorded at one or multiple points in the apparatus. The embedding method is a way to reconstruct a representation of the attractor from the scalar observations. The reconstruction has the same topology as the attractor if the embedding dimension is selected properly. According to the embedding theorem, if a set of scalar measurements $\{v(t)\}$ is given, a set of vectors $\{X(t)\}$ can be formulated by

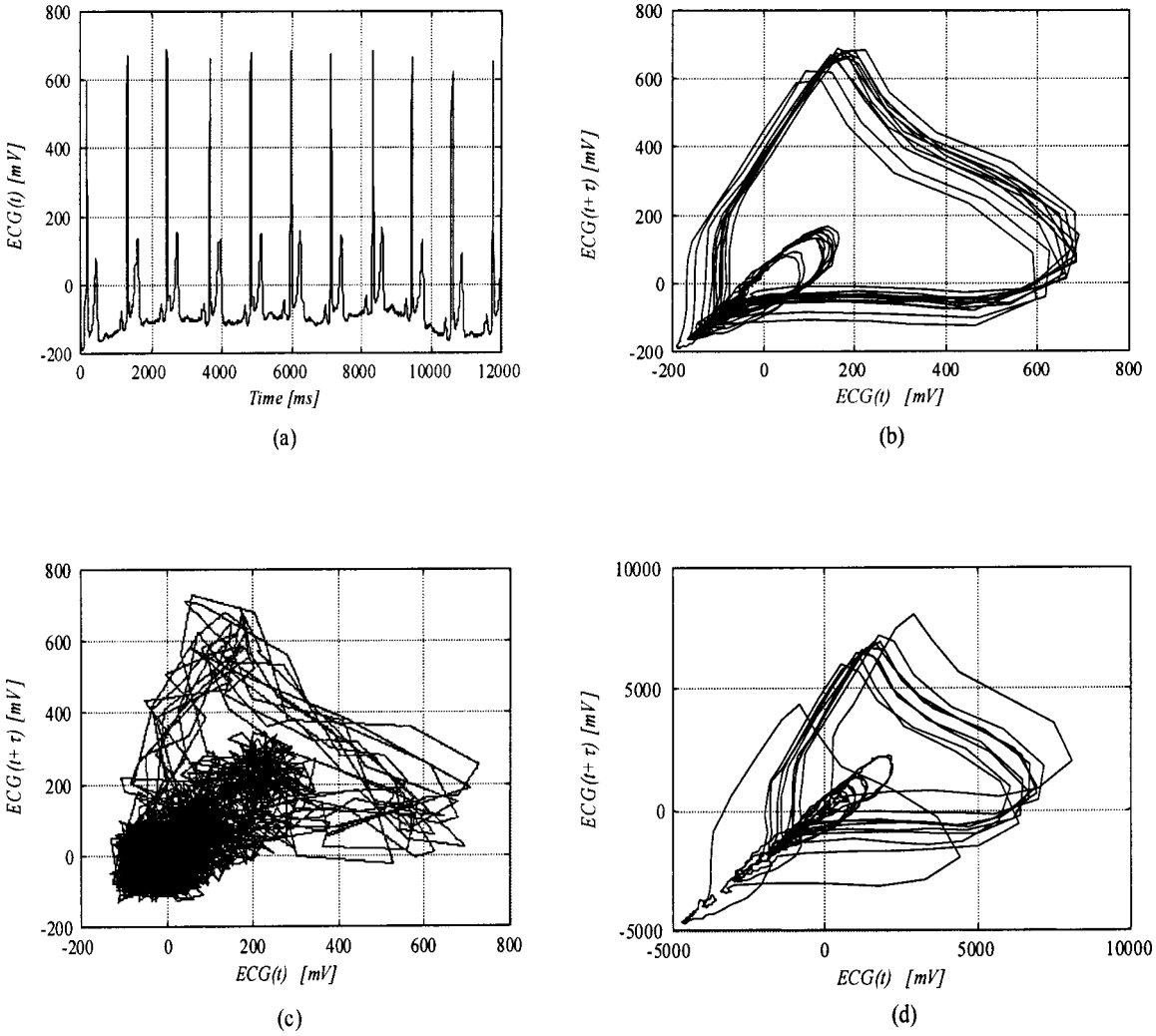

FIGURE 2. The effect of noise in reconstructing the phase portraits of ECG: (a) sampled (unfiltered) ECG signal; (b) phase portrait of sampled ECG signal; (c) phase portrait of ECG signal corrupted with severe, high frequency muscle contraction noise; (d) phase portrait of ECG signal corrupted with low frequency baseline shifts on.

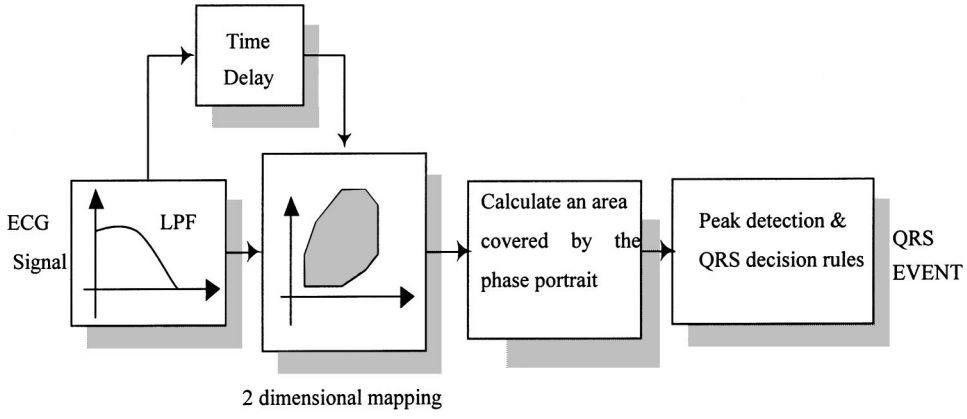

FIGURE 3. A block diagram of our proposed QRS detection algorithm. First, the ECG signal is filtered by low-pass filter to remove high-frequency noise components. The filtered ECG signal is mapped into two-dimensional consecutive vector space. To detect QRS complex peaks, the area covered by phase portrait of ECG signal is calculated. Based on these computed values, the candidate points of QRS complex are extracted. Then, those selected candidate points are processed by the decision rules to identify as the QRS complex.

$$X(t)=\begin{pmatrix} v(t) \\ v(t+\tau) \\ \vdots \\ v[t+\tau\cdot(d_m-1)] \end{pmatrix}, \qquad (1)$$

where τ is a time delay and d_m is a mapping dimension. In mathematical terms, the embedding mapping is continuous, one-to-one, and reversible. To ensure the existence of a topological mapping from the original vector space to the embedding one, the mapping dimension d_m is set to be $d_m \geqslant 2n+1$.[21] Here, n is the dimension of data in the original space but this strict constraint is reduced significantly.[22,23] In our application, we did not stick to this regulation since we considered the embedding space as a discrete and nonreversible delay-coordinate mapping. We referred to the set of vectors $\{X(t)\}$ as a ''phase portrait'' and adopted an embedding method as two-dimensional delay-coordinate mapping. A phase portrait of the ECG signal can be constructed from a set of scalar measurements introducing a time delay τ that leads to the $v(t), v(t+\tau), v(t+2\tau), \ldots, v[t+(m-1)\tau]$ vectors, where m is a mapping dimension. Figure 1 shows the phase portraits of the ECG signal with varying time delay τ. To reconstruct the phase portraits, we fixed a mapping dimension as 2 since this mapping dimension is almost sufficient to reproduce the attractor. From Fig. 1, we can see that a reconstructed phase portrait depends on the amount of time delay. If the time delay τ is properly selected, the peaks of ECG signal (P, T, and QRS complexes) are easily recognized as shown in Fig. 1(c). In Fig. 1(b), the time delay is set to be 8 ms. This value seems to be rather small since the resulting trajectories in phase space domain take place on the diagonal axis of the space ($y=x$). In Fig. 1(c), the time delay is properly chosen to 20 ms. The phase portrait of ECG signals is clearly and widely distributed over the space. In Fig. 1(c), we could notice that the outer trajectories corresponded to ventricular contraction, i.e., QRS complex and inner small trajectories corresponded to P or T wave, respectively. Hence the relationship between ECG wave components and trajectories makes it possible to discriminate the QRS complex from ECG wave components. In Fig. 1(d), the time delay is set to be 40 ms. We could also notice that the excessive time delay caused the phase portraits to overlap each other and to be disjointed by stretching and folding. As seen in Fig. 1, the mapping parameters play important roles for shaping a phase portrait of QRS complexes. Thus we should select the mapping parameters with discretion. Moreover, real-time processing must be considered to reduce the additional preprocessing stages or computation times. From our observations, we could infer that the geometrical property of phase portraits could be utilized as a detection measure of the QRS complex.

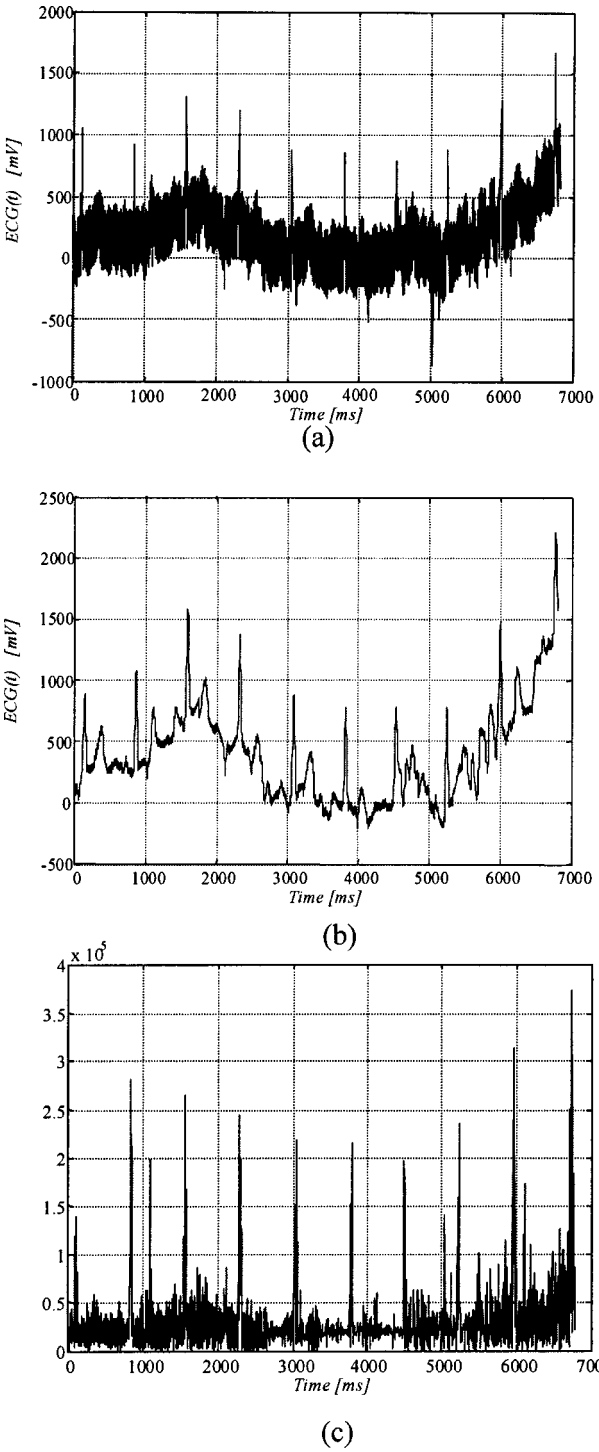

FIGURE 4. Output waveforms from each processing step of QRS detection algorithm: (a) typical ECG signal; (b) low pass filtered ECG signal; (c) an area of the phase portrait covered by the filtered ECG signal.

Relationship Between Noises and the Reconstructed Phase Portrait of ECG Signal

Noise components in ECG signals make trajectories obscure and hard to recognize their structures from the

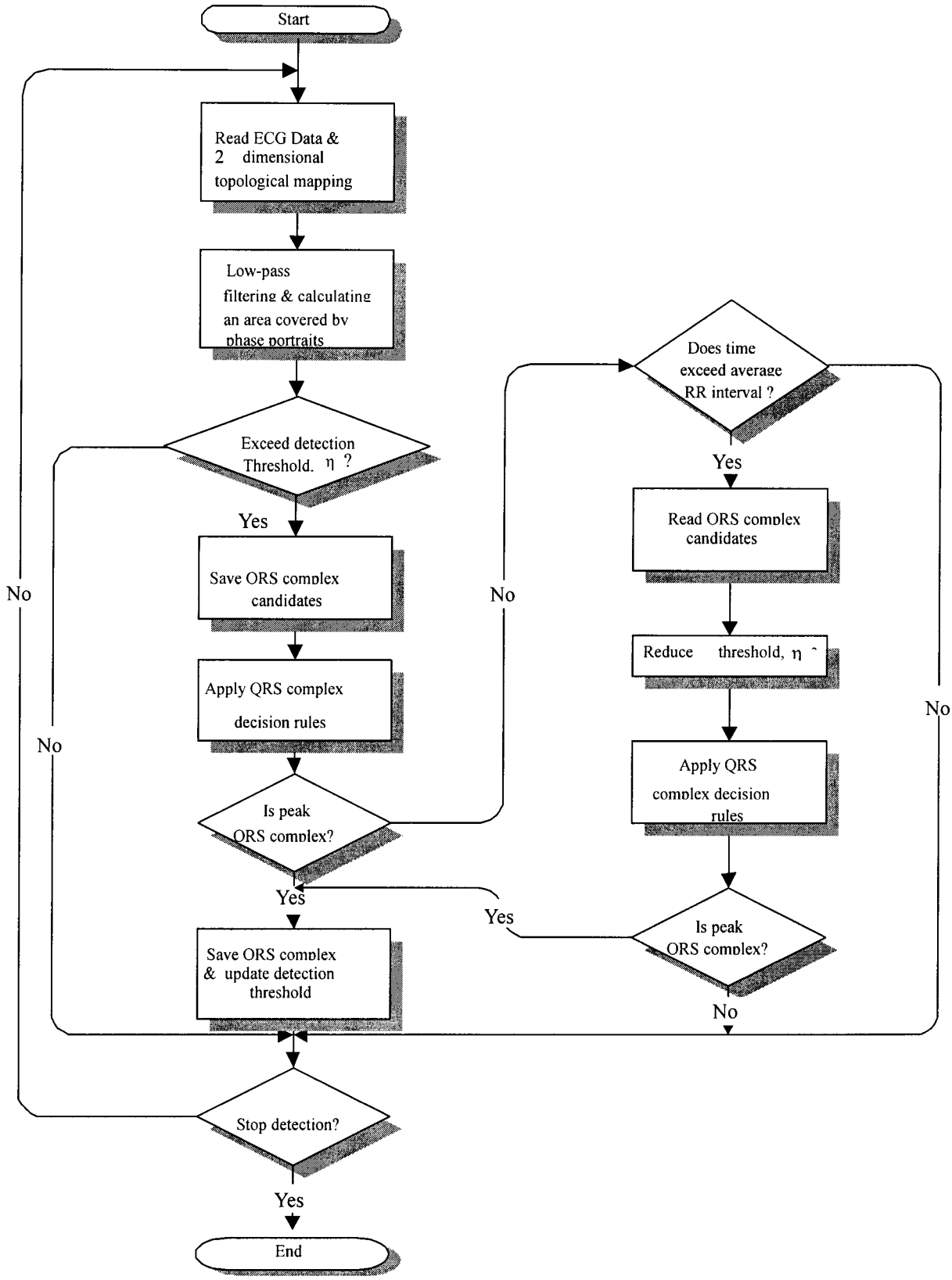

FIGURE 5. A flow chart for describing proposed QRS complex detection algorithm.

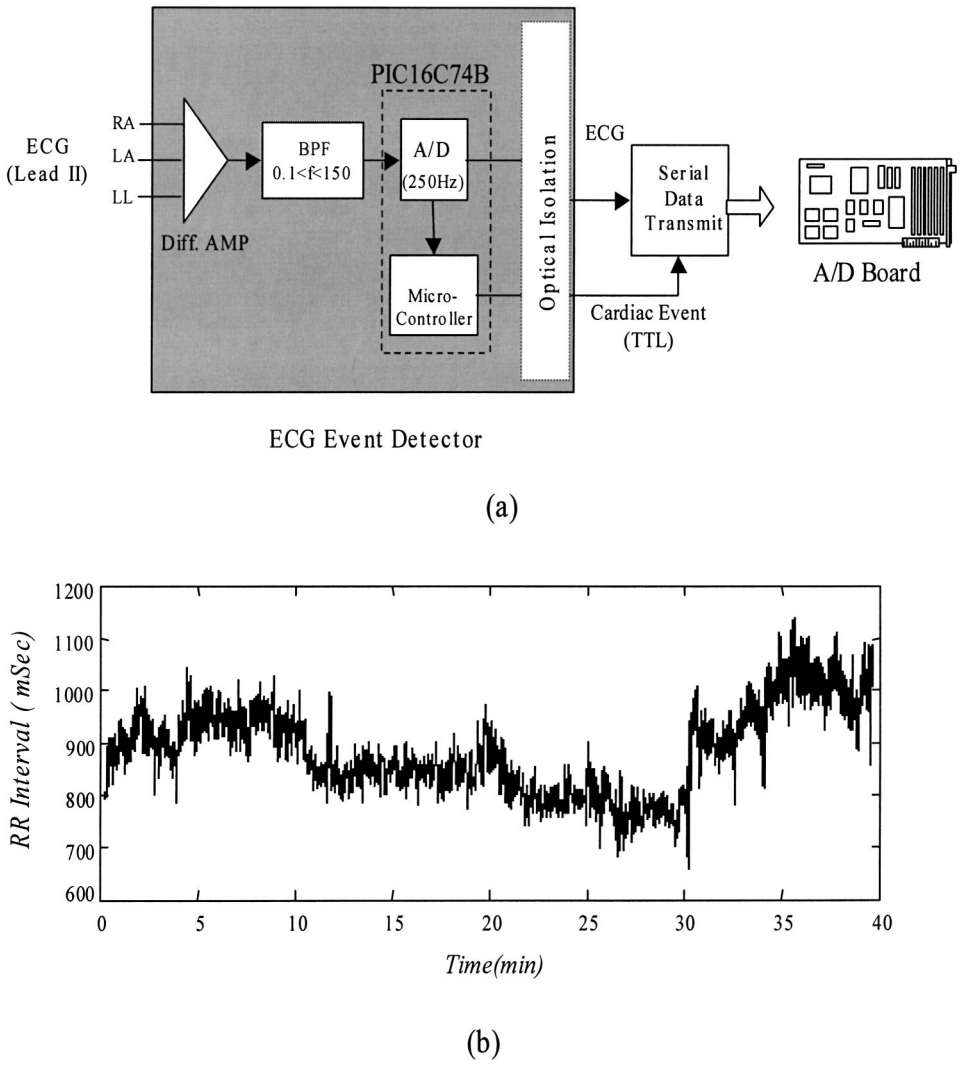

FIGURE 6. A hardware implementation of proposed algorithm with a microcontroller: (a) system configuration; (b) output of the system identifying QRS complex as R–R interval tachogram.

reconstructed phase portrait from ECG signals. Khan[10] raised this issue and emphasized the importance of inventing a reliable technique for efficiently handling noisy components of ECG signals. In Fig. 2, we could observe the effect of noise contamination such as power line interference, electrode contact noise, high frequency banded muscle contraction [Fig. 2(c)], base-line drift, or low frequency banded noise due to respiration [Fig. 2(d)]. For the case of low frequency noise contamination, phase portrait structure was clearly recognized but if a peak level of high-frequency noise exceeds a certain threshold level, phase portrait structure is severely distorted and consequently the meaningful geometrical features can be barely recognized. Hence, it is very crucial to reduce high-frequency banded noise components from ECG signals. To do this, a low-pass preprocess filter is applied to ECG signals to reduce high-frequency noise.

METHODS

Preprocessor

As a preprocessor, multiple filtering stages using linear or nonlinear transformations have usually been applied to localize the QRS complex. All of the preprocessors[3,6,16,17,19,28] consist of at least three or more filtering steps before applying any decision rule to detect QRS complexes. Figure 3 illustrates a block diagram of our proposed QRS detection algorithm. For the preprocessor, we use a single low-pass filter with a cutoff frequency of 20 Hz to remove high-frequency components irrelevant of the QRS complex spectral components. As high-frequency noise degrade trajectory precision drawn in the mapping space, the following second ordered low-pass filter[8] is used as a preprocessor:

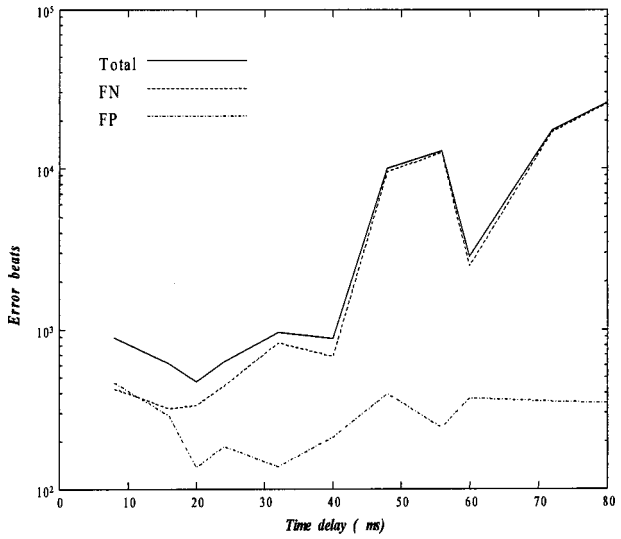

FIGURE 7. QRS complex detection error with the various time delays. The dimension of topological mapping is fixed to 2.

$$y(nT)=2y(nT-T)-y(nT-2T)+x(nT) \\ -2x(nT-6T)+x(nT-12T), \qquad (2)$$

where T is the sampling period and n is an arbitrary integer. After low-pass filtering is applied, the filtered ECG sequences are mapped into two-dimensional consecutive vector space, $\{\xi(n):y[nT],y[(n-\tau)T]\}$ where τ is a time delay.

R Peak Detection

As mentioned previously, the geometrical property of phase portrait, i.e., lag rotundity can be utilized as the QRS complex detection factor. Moreover, if time delay τ is properly chosen, the phase portrait of ECG signal forms the largest attained area on phase space domain can be utilized as a QRS detection criterion. We use vector algebra to calculate an area covered by the consecutive vector space. The displacement vector is defined by

$$\mathbf{D}(n)=\begin{bmatrix} \xi(n)-\xi(n-1) \\ \xi(n-1)-\xi(n-2) \\ \vdots \\ \xi[n-(d-1)]-\xi(n-d) \end{bmatrix}, \qquad (3)$$

where d is the dimension of displacement vector. In our study, d is limited to 10. This restriction is based on the fact that if average QRS duration is less than 90 ms,[14]

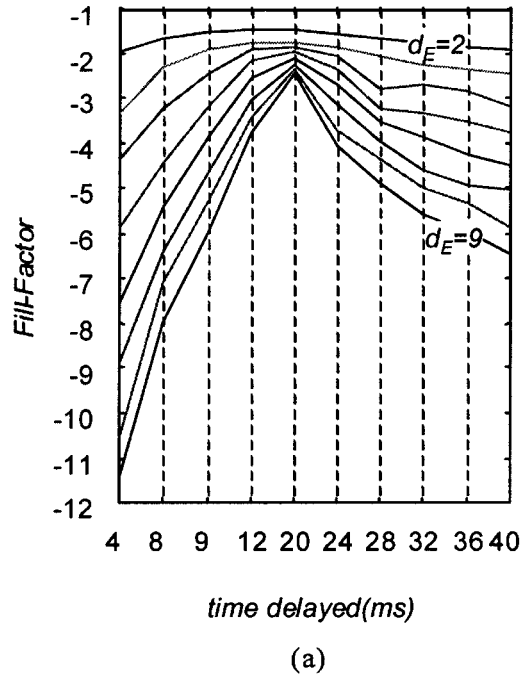

(a)

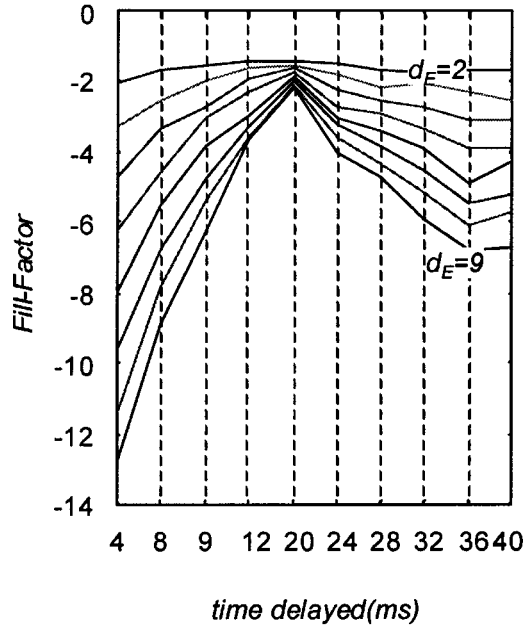

(b)

FIGURE 8. The results of fill-factor algorithm applying on (a) tape No. 201, and (b) tape No. 205, respectively.

the sample points comprising of vector loops made by QRS complex are within this limit. If we consider the elements of Eq. (3) as the edges of polygon, we could calculate an area of the polygon[11] by simply evaluating a determinant from Eq. (3):

$$V(n)=\det|\mathbf{D}(n)|. \qquad (4)$$

TABLE 1. Estimation of time delay in two-dimensional space. First 10 min episode of all MIT/BIH arrhythmia database (except transitional margin 3 min from the start of each file) were used to estimate time delay.

Estimation methods	Estimated average delay (ms)
Mutual information	28 ± 3.51
Fill factor	20 ± 0.76

The QRS complex can be observed as a maximum value of $V(n)$. To do this, we first compute a left and right local quantitative variation LLV_n, RLV_n with nth candidate point such that

$$LLV_n = V(n) + V(n-1), \quad RLV_n = V(n) + V(n+1). \tag{5}$$

The absolute value of these values are compared with the first threshold value η_1:

$$\left| \sum_{i=n-1}^{n+1} LLV_i \right| \geq \eta_1 \quad \text{AND} \left| \sum_{i=n-1}^{n+1} RLV_i \right| \geq \eta_1. \quad \text{(Case I)} \tag{6}$$

If Eq. (6) holds, the candidate point is classified as a new QRS complex. Otherwise, the following second comparison is made with respect to the second threshold value η_2 by

$$\left| \sum_{i=n-1}^{n+1} LLV_i \right| \geq \eta_2 \quad \text{OR} \left| \sum_{i=n-1}^{n+1} RLV_i \right| \geq \eta_2. \quad \text{(Case II)} \tag{7}$$

If the logical OR in Eq. (7) is true, the considered candidate point is also classified as a new QRS complex. However, if Eq. (7) is failed, the candidate point is discarded and Eqs. (5), (6), and (7) are considered iteratively with $(n+1)$th candidate point $V(n+1)$. The threshold values η_1, η_2 are updated whenever a new QRS complex is detected such that

$$\eta_1, \eta_2 = \text{the average value of last updated 2 or 3 } \eta_{\text{MIN}_{\text{region}}}, \tag{8}$$

$$\eta_{\text{MIN}_{\text{region}}} = \frac{(\eta_{\text{MAX}} + \eta_{\text{MIN}})}{2}, \tag{9}$$

$$\eta_{\text{MIN}} = \text{MIN}[LLV_Q, RLV_Q],$$

$$\eta_{\text{MAX}} = \text{MAX}[LLV_Q, RLV_Q], \tag{10}$$

$$LLV_Q = \{LLV_{\text{QRS}\_i} : i = 1-5\},$$

$$RLV_Q = \{RLV_{\text{QRS}\_i} : i = 1-5\}, \tag{11}$$

where LLV_{QRS} and RLV_{QRS} are the left and right local quantitative variation values when a new QRS complex is considered. LLV_Q and RLV_Q are the five pairs of LLV_{QRS} and RLV_{QRS} values, respectively, with considering the four previously detected QRS complexes.

In order to improve the QRS complex detection rate, the following decision rules are also considered:

(1) *Refractory blanking rule:* Any QRS event within 200 ms followed by the detected QRS complex is ignored due to the physiological constraint imposed by a refractory period on a cardiac muscle.
(2) *Search back rule:* If no QRS detection occurs within 150% of the latest mean RR interval, a new QRS search is attempted by applying 80% and 50% of the previous threshold values η_1 and η_2, respectively.

In Fig. 4, a typical ECG and the resulting output waveforms from each stage are illustrated. A flow chart for describing our proposed algorithm is shown in Fig. 5.

Hardware Implementation

We applied our algorithm to devise a real-time QRS detection system for analyzing HRV acquired from 48 subjects. First we implemented the QRS detection algorithm on a conventional 8-bit microcontroller with A/D converter (Microchips, PIC16C74B, 4 MHz). Through this hardware, the acquired ECG signals from a subject were sampled at 4 ms with 8-bits resolution A/D converter. The detection algorithm was written in C language, and programmed into 4 K bytes of internal ROM. The working area in RAM was 192 bytes. Figure 6 shows a configuration of system and R–R interval records during our experiment. The system was developed to record 1 h cardiovascular signals such as ECG, respiration, and blood flow to investigate HRV characteristics of the patients with vasovagal syncope. An ECG event indicating board was located at a patient's side. The outputs of ECG event indicating board were ECG and TTL level event signal corresponded to the QRS complex. The ECG and event signals were recorded by a personal computer using A/D board and saved for the future processing. In our experiment, it turns out that the proposed QRS detection algorithms accurately detect QRS complex in normal or noisy environment.

RESULTS

The mapping parameters, time delay and mapping dimension affect phase portraits of the ECG signal. We

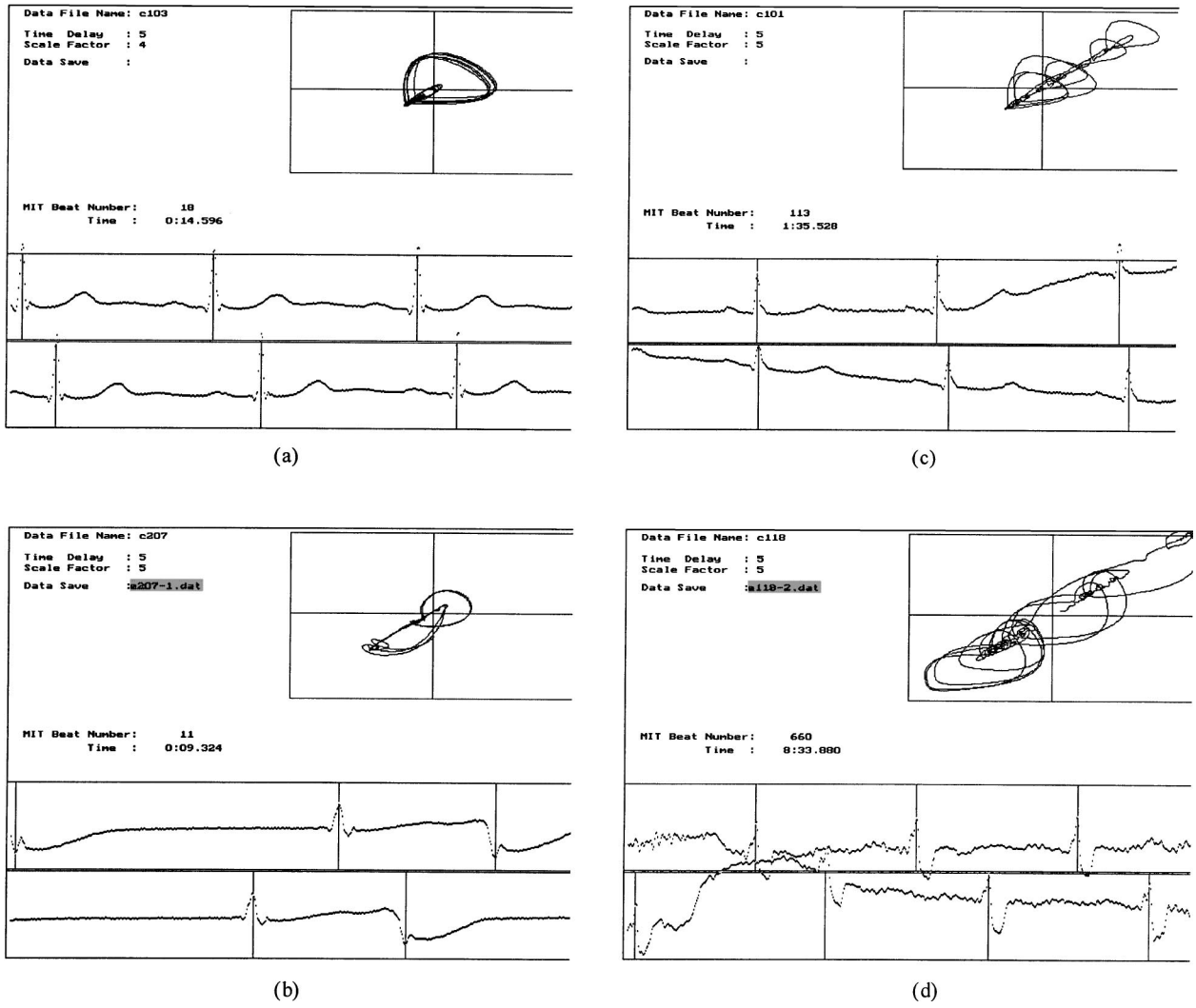

FIGURE 9. Screen snap shots of our proposed QRS detection program: (a) normal ECG signal (tape No. 103), ECG signals containing (b) irregular QRS complex pattern (tape No. 207), (c) base-line drift pattern (tape No. 101), (d) base-line drift and muscle contraction noise. Each phase portrait of ECG signal was depicted on the right top of each screen, respectively.

choose the mapping dimension as 2 to reduce the computational time and additional processing steps. To find a proper time delay, we applied QRS detection algorithm to MIT/BIH arrhythmia database[15] containing the various time delays. Figure 7 shows the results of our experiment. In Fig. 7, we can find that the most suitable time delay is 20 ms but we cannot find any other valuable information from the relationship between the mapping dimension and the time delay since we fix a mapping dimension as 2. To investigate this relationship further, many researchers had adopted nonlinear dynamics.[2,4,9,13,24,25] In contrast, this research mainly investigated the chaotic characteristics of the dynamic system, our study tried to interpret the meaning and resolve the relationship between the phase portrait of QRS complex and mapping parameters. To meet our requirements, we applied a fill-factor[13] and mutual information algorithm[4] successively. A fill-factor method provides an optimal utilization index of embedding space reconstructed by phase portraits whereas mutual information algorithm provides information about the independence of two variables. Figure 8 shows the result after applying a fill-factor algorithm to tape No. 201 and tape No. 205 of MIT/BIH arrhythmia database, respectively. The first 10 min episode except transitional margin 3 min from the actual start of each MIT/BIH arrhythmia database file was used. In Fig. 8, as a mapping dimension d_m increases, a local maximum is clearly visible with 20 ms time delay. This means that if two successive vectors are 20 ms apart, the phase portrait comprised of two vectors are maximally utilizing the vector space, that is, the area covered by the vector loop is the most spacious. Since the higher mapping dimension does not affect the utilization index of mapping

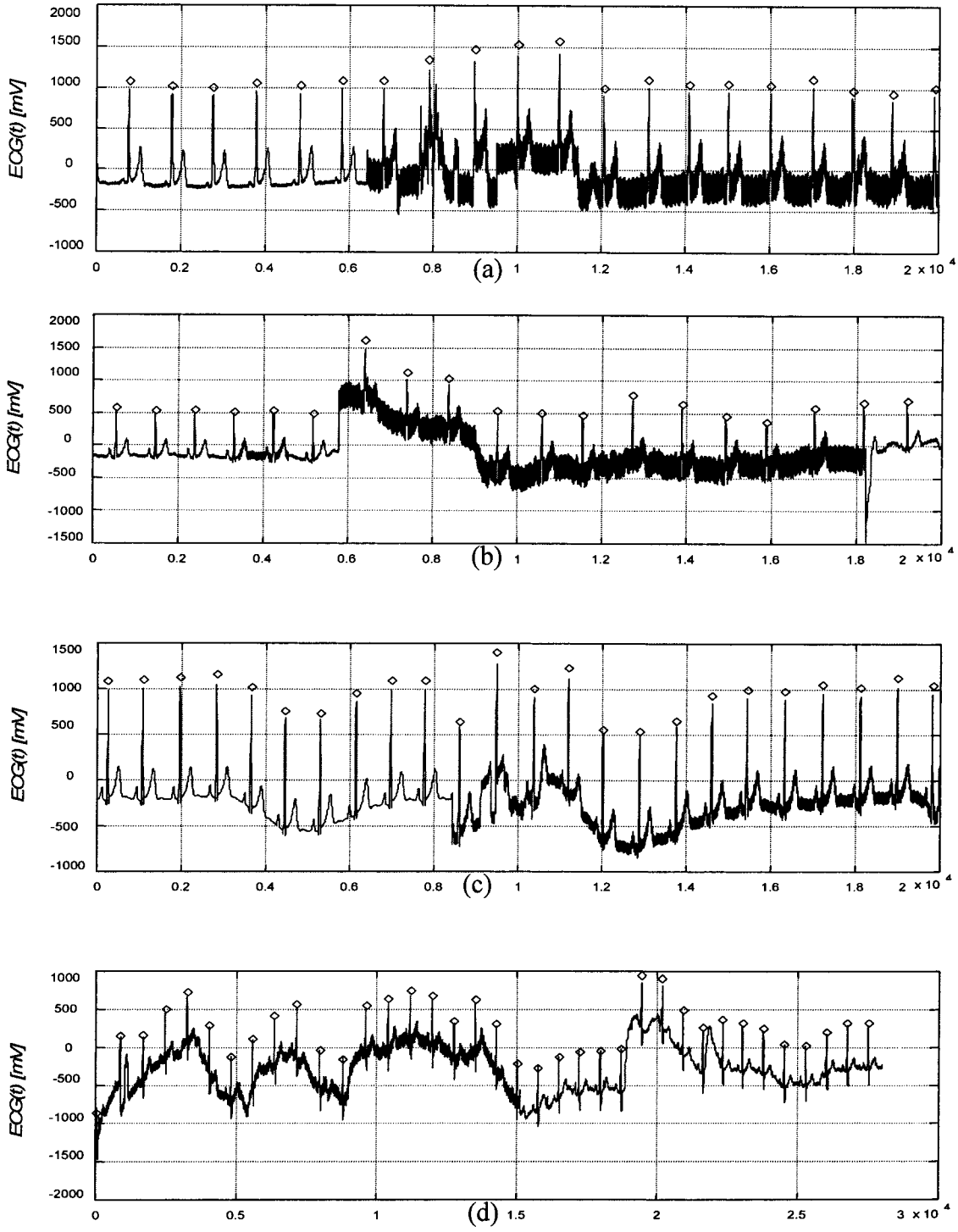

FIGURE 10. Results of applying our QRS detection algorithm. The symbol (◇) marks a location of R peaks: (a) and (b) contain muscle contraction noise whereas (c) and (d) contain baseline shifts one.

space, we fixed a mapping dimension to 2 to reduce processing time and computational burden of a small microcontroller. The estimated time delay in two-dimensional mapping space is summarized in Table 1. Figures 9 and 10 illustrate the results of our QRS detection program executed on a 486 IBM PC. The reconstructed phase portrait from ECG signal was shown on the right top of screen. Table 2 summarizes the detection performance of our proposed algorithm with applying 20 ms time delay to MIT/BIH database.

TABLE 2. The performance of proposed QRS complex detection algorithm.

Tape No.	Total (beats)	FP (beats)	FN (beats)	Failed detection FP+FN (beats)	Failed detection (FP+FN)/ Total (%)
100	2272	0	0	0	0.00
101	1865	2	0	2	0.11
102	2187	0	3	3	0.14
103	2084	0	0	0	0.00
104	2228	0	0	0	0.00
105	2572	41	4	45	1.75
106	2027	2	0	2	0.10
107	2137	0	2	2	0.09
108	1763	9	11	20	1.13
109	2532	0	0	0	0.00
111	2124	0	1	1	0.05
112	2539	0	0	0	0.00
113	1794	1	0	1	0.06
114	1878	0	40	40	2.13
115	1953	0	0	0	0.00
116	2412	1	19	20	0.83
117	1535	0	0	0	0.00
118	2278	1	0	1	0.04
119	1987	2	0	2	0.10
121	1862	0	1	1	0.05
122	2476	1	0	1	0.04
123	1518	0	0	0	0.00
124	1619	0	0	0	0.00
200	2601	13	1	14	0.54
201	1963	0	27	27	1.38
202	2136	0	1	1	0.05
203	2980	25	47	72	2.42
205	2656	0	2	2	0.08
207	1860	0	17	17	0.91
208	2955	12	21	33	1.12
209	3004	1	0	1	0.03
210	2650	3	23	26	0.98
212	2748	0	0	0	0.00
213	3250	1	1	2	0.06
214	2261	1	2	3	0.13
215	3363	0	0	0	0.00
217	2208	2	6	8	0.36
219	2154	4	10	14	0.65
220	2048	0	0	0	0.00
221	2427	0	0	0	0.00
222	2483	5	91	96	3.87
223	2605	0	0	0	0.00
228	2053	7	5	12	0.58
230	2256	2	0	2	0.09
231	1571	0	0	0	0.00
232	1780	1	0	1	0.06
233	3079	0	0	0	0.00
234	2753	0	0	0	0.00
Total	109481	137	335	472	0.42

DISCUSSION

Table 2 shows that the evaluation of our algorithm on MIT/BIT arrhythmia database produces 137 false positive (FP) beats (99.87% positive predicable rate) and 335 false negative (FN) beats (99.57% sensitivity) with a total detection failure of 472 beats (error rate of 0.42%). In Table 3, the performance of our topological mapping QRS detector is compared with Hamilton–Tompkins,[6] Wavelet,[12] and Wavelet-DSP,[5] respectively. For the comparisons, we selected the several tapes such as tape Nos. 105, 108, 201, 203, 222, and 228. tape No. 105 contains a high amount of noise and artifacts. In tape No. 108, there exists first-degree of borderline arterial ventricle (AV) blocks, fusion premature ventricular contractions (PVCs), and also severe time-varying morphological changes. In tape No. 201, time-varying morphological changes, such as uniform PVCs, ventricular trigeminy, and super ventricular tachyarrhythmias with aberration (SVTA) exist. In tape No. 203, PVCs are multiformed and QRS morphological changes exist. Also, there is considerable noise including muscle artifact and baseline shift. Hence it is very difficult for ECG to detect QRS complexes from evaluating tape No. 203. For tape No. 222, it is characterized by arterial flutter/fibrillation and the occurrences of high-frequency noise on the several intervals, and multiformed PVCs. The short occurrence of tape slippage characterizes tape No. 228. Table 3 compares the QRS detection performance of six selected tapes from MIT/BIH database for each algorithm. In overall error rate, wavelet algorithm exhibits the best performance because it efficiently adapts to the variations of QRS morphology. In tape Nos. 108, 201, and 222, our proposed algorithm exhibits the worst performance. For these three files, time-varying morphological change, severe high-frequency noise, and the occurrence of tape slippage distort the area attained by phase portraits. Due to the unpredictable trend of ECG wave morphology and R–R intervals, the biologically based detection estimator such as time-frequency analysis and wavelet transform are more feasible for the accurate QRS detection but, for a portable device where a small microcontroller is required, our proposed algorithm is the most feasible solution in terms of code size and efficiency.

CONCLUSION

One of the specific properties of our algorithm is transforming signal domain space from one-dimensional sampled ECG signal into two-dimensional phase portraits by introducing lag-coordinate mapping. To detect the QRS complex, we utilized the geometrical property of phase portraits, i.e., lag rotundity. For a real-time computation with a microcontroller implementation, our proposed QRS detection algorithm uses integer arithmetic and two-dimensional mapping since these constraints are feasible in a micro-controller application. Unlike the previous works[3,6,16,17,19,26] our algorithm could eliminate some unnecessary preprocessing filter stages. But like the other QRS detection algorithm, the overall

TABLE 3. A comparison of topological mapping QRS complex detection with Hamilton–Tompkins, wavelet, wavelet DSP.

		Algorithm on MIT/BIH arrhythmia database											
		Topological mapping overall error: 0.42%			Wavelet-DSP overall error: 0.26%			Wavelet overall error: 0.15%			Hamilton–Tompkins overall error: 0.54%		
Tape No.	No. Beats	FP	FN	Error (%)	FP	FN	Error (%)	FP	FN	Error (%)	FP	FN	Error (%)
105	2572	41	4	1.75	27	15	0.63	15	13	1.09	53	22	2.95
108	1763	9	11	1.13	20	29	2.78	13	15	1.59	50	47	5.67
201	1963	0	27	1.38	7	24	1.07	1	12	0.66	3	19	1.14
203	2980	25	47	2.42	11	21	1.12	2	24	0.87	14	61	2.57
222	2483	5	91	3.87	12	27	1.57	1	9	0.40	40	37	3.14
228	2053	7	5	0.58	11	23	1.65	3	7	0.49	19	6	1.22

performance is highly depended on the ability of estimation of signal peaks. Our proposed algorithm did not affected by the processing time because it fixed detection delay as 50–90 ms and consisted of simple procedures. As this is the case, our proposed real-time QRS detection algorithm can be easily implemented with a microcontroller to produce the efficient results for a real application such as portable or ambulatory ECG monitor.

REFERENCES

[1] Babloyantz, A., and A. Destexhe. Is the normal heart a periodic oscillator? *Biol. Cybern.* 58:203–211, 1988.

[2] Broomhead, D. S., and J. P. King. Extracting qualitative dynamics from experimental data. *Physica D* 20:217–236, 1986.

[3] Dandapat, S., and G. C. Ray. Spike detection in biomedical signals using midprediction filter. *Med. Biol. Eng. Comput.* 35:354–360, 1997.

[4] Fraser, A. M., and H. L. Swinney. Independent coordinates for strange attractors from mutual information. *Phys. Rev. A* 33:1134–1140, 1986.

[5] Hahoura, M., M. Hassani, and M. Hubin. DSP implementation of wavelet transform for real time ECG wave forms detection and heart rate analysis. *Comput. Methods Prog. Biomed.* 52:35–44, 1997.

[6] Hamilton, P. S., and W. J. Tompkins. Quantitative investigation of QRS detection rules using the MIT/BIH arrhythmia database. *IEEE Trans. Biomed. Eng.* BME-33:1157–1187, 1986.

[7] Kadambe, S., R. Murray, and G. F. Boudreaux-Bartels. Wavelet transform-based QRS complex detector. *IEEE Trans. Biomed. Eng.* 46:838–848, 1999.

[8] Kaplan, D. T., and R. J. Cohen. Is fibrillation chaos? *Circ. Res.* 67:886–892, 1990.

[9] Kember, G., and A. C. Fowler. A correlation function for choosing time delays in phase reconstructions. *Phys. Lett. A* 179:72–80, 1993.

[10] Khan, S., T. A. Denton, H. S. Karagueuzian, and G. A. Diamond. Effect of noise and filtering on phase plane plots and dimension for simple periodic signals. *Ann. Int. Conf. IEEE EMBS* 13:2232–2233, 1991.

[11] Kreyszig, E. Advanced Engineering Mathmatics, 6th ed., New York: Wiley, 1988, p. 306.

[12] Li, C., and C. Zheng. Detection of ECG characteristic points using wavelet transform. *IEEE Trans. Biomed. Eng.* 42:21–28, 1995.

[13] Liebert, W., K. Pawelzik, and H. G. Schuster. Optimal embeddings of chaotic attractors from topological consideration. *Europhys. Lett.* 14:521–526, 1991.

[14] Macfarlane, P. W., and T. D. V. Lawrie, Comprehensive Electrocardiology: Theory and Practice in Health and Disease, New York: Pergamon, 1989, Vol. 1, p. 435.

[15] MIT/BIH Database Distribution, Massachusetts Inst. Technol., 77 Massachusetts Avenue, Room 20A-113, Cambridge, MA 02139.

[16] Okada, M. A digital filter for the QRS complex detection. *IEEE Trans. Biomed. Eng.* BME-26:700–703, 1979.

[17] Pan, J., and W. J. Tompkins. A real-time QRS detection algorithm. *IEEE Trans. Biomed. Eng.* BME-32:230–236, 1985.

[18] Richter, M., T. Schreiber, and D. T. Kaplan. Fetal ECG extraction with nonlinear state-space projections. *IEEE Trans. Biomed. Eng.* 45:133–136, 1998.

[19] Ruha, A., S. Sallinen, and S. Nissilä. A real-time microprocessor QRS detector system with a 1 ms timing accuracy for the measurement of ambulatory HRV. *IEEE Trans. Biomed. Eng.* 44:159–167, 1997.

[20] Sahambi, J. S., S. N. Tandon, and R. K. Bhatt. Wavelet based ST-segment analysis. *Med. Biol. Eng. Comput.* 36:568–572, 1998.

[21] Sauer, T. D., J. A. Yorke, and M. Casdagli. Embedology. *J. Stat. Phys.* 65:579, 1991.

[22] Sauer, T. D., and J. A. Yorke. How many delay coordinated do you need? *Int. J. Bifurcation and Chaos* 3:737, 1993.

[23] Sauer, T. D., and J. A. Yorke. Are the dimension of a set and its image equal under typical smooth functions? *Ergodic Theory Dyn. Sys.* 17:941–956, 1997.

[24] Schuster, H. G. Deterministic Chaos. Weinheim: VCH, 1988.

[25] Schuster, H. G., and W. Liebert. Proper choice of the time delay for the analysis of chaotic time series. *Phys. Lett. A* 142:107–111, 1989.

[26] Shaw, R. S. Strange attractor, chaotic behavior and information flow. *Nature (London)* 36a: 1980.

[27] Takens, F. Lecture Notes in Mathematics, Berlin: Springer, 1980, Vol. 898, p. 230.

[28] Xue, O., Y. H. Hu, and W. J. Tompkins. Neural-network-based adaptive matched filtering for QRS detection. *IEEE Trans. Biomed. Eng.* BME-39:317–329, 1992.